Energy Proceedings
Vol 56, 2025
ISSN 2004-2965

Study on the Regulation of Nanostructure on Wettability of CO_2 Droplets on Substrate: Molecular Dynamics Simulation

Hengguang Cao[1], Xuewen Cao[1*], Jiang Bian[2]

1 College of Pipeline and Civil Engineering, China University of Petroleum (East China), Qingdao, China

2 School of Petroleum Engineering, Yangtze University, Wuhan, China
(*Corresponding Author: caoxw@upc.edu.cn)

ABSTRACT

This study employs molecular dynamics simulations to investigate how nanostructures influence the wetting behavior of CO_2 droplets by varying the solid–liquid interaction coefficient (α), surface feature size, and surface configuration. The results reveal that increasing α drives the transition of droplets from the Cassie state to the Wenzel state. Under identical α, the contact angle on square pillar surfaces is larger than on smooth surfaces. Notably, at α = 0.14, introducing a pillar structure can switch the surface from CO_2-philic to CO_2-phobic. Further modifications in pillar height and solid fraction induce a Wenzel-to-Cassie transition, significantly increasing the contact angle and reducing CO_2–surface interaction energy. Surfaces featuring square pillars, cylinders, or grooves exhibit similar effects in tuning droplet wetting. These insights provide valuable guidelines for optimizing materials and surface designs to enhance CO_2 condensation and liquefaction efficiency.

Keywords: Carbon dioxide, nanostructure, wettability, contact angle, wetting state

NONMENCLATURE

Abbreviations	
CO_2	Carbon Dioxide
FCC	Face-centered cubic
LJ	Lennard-Jones
MD	Molecular dynamics
Symbols	
H	Pillar height
q	Charges carried by the atom
r_{ij}	Distance between two particles
S	Side length
T	Spacing of the groove structure
F	Solid fraction
α	Solid–liquid interaction coefficient
ε	Depth of the potential well
ε_0	Vacuum permittivity
σ	Equilibrium distance
Φ	Diameter of he cylinder structure

1. INTRODUCTION

CO_2 is one of the main anthropogenic greenhouse gases[1], and emissions caused by industrialization and fossil fuel consumption are intensifying global warming, posing a potential threat to human survival and creation. Recently, major efforts have been made in carbon capture [2] and storage [3] from fixed sources and in developing clean energy [4] to reduce anthropogenic CO_2 emissions, thus slowing and reversing the process of global warming [5]. Among these, carbon capture, utilization, and storage (CCUS) technology [6] has garnered significant attention, as it captures CO_2 emissions from fossil fuel power generation and industrial processes for reuse or sequestration [7], and is considered one of the most effective strategies to combat CO_2 emissions [8]. The liquefaction of CO_2 is a key processing step in CCUS technology [9],[10]. Once liquefied, CO_2 significantly reduces in volume, making it easier to transport over long distances and in large quantities via pipelines, ships, and other means. This not only reduces transportation costs but also enhances transportation efficiency [11],[12]. Additionally, liquid CO_2 is safer during storage and transportation compared to gaseous CO_2 [13]. During the liquefaction process, the wetting behavior of CO_2 droplets on heat exchange surfaces directly impacts condensation and heat transfer efficiency [14]. Therefore, understanding the wetting behavior of CO_2 droplets on

---

This is a paper for International CCUS Conference 2024 (ICCUS 2024), June 20-22, 2024, Beijing, China.

heat exchange surfaces [15] is fundamental to grasping the mechanisms of CO_2 condensation and heat transfer, aiding in better controlling the condensation process [16], optimizing the liquefaction process, and promoting the broad application of CCUS technology.

Wettability refers to the ability or tendency of a liquid to spread on a solid surface [17], which is mainly determined by the characteristic interaction energy between the droplet and the surface [18], the morphology of the solid surface [19], and the presence of external fields [20], and is commonly described by the contact angle. Based on the contact angle of droplets on the surface, surfaces can be classified into hydrophilic and hydrophobic surfaces, and designing material surfaces with different wettabilities can meet diverse engineering requirements [21]. For smooth surfaces, increasing surface hydrophobicity to obtain larger contact angles is mainly achieved by reducing the surface energy of the solid surface, i.e., by altering the chemical composition of the surface [22]. Due to the lack of need for external energy input and lower material property requirements, the advantages of controlling droplet wettability by altering the surface microstructure are becoming increasingly prominent [23]. There are primarily two wetting states for droplets on structured surfaces: the Wenzel state and the Cassie state [24]. In the Wenzel state, droplets fully wet the structured surface, filling the surface voids. Conversely, in the Cassie state, droplets only wet the tops of the surface protrusions. Additionally, there is a partially wetted PW state where droplets only infiltrate part of the structural gaps [25].

The Wenzel state and Cassie state, the two typical wetting states, each have their pros and cons in the field of heat and mass transfer. The larger solid-liquid contact area in the Wenzel state enhances heat transfer between the droplet and the surface, but it also results in a more significant adhesion effect [26]. Although the vapor within the surface structure gaps in the Cassie state provides the droplet with excellent mobility, it also increases the thermal resistance for heat transfer between the droplet and the solid surface [27]. Many researchers have investigated the transition of droplet wetting states on structured surfaces [28],[29]. Wu et al. [30] studied the wetting behavior of R32, R1234yf, and R32/R1234yf nanodroplets on square pillar substrates. When the structure height is constant, with larger structure spacing, the droplet wetting state tends toward the Wenzel state. When the structure spacing is fixed, with higher structure height, the droplet wetting state tends toward the Cassie state. Additionally, within the studied structures, the position of the wetting state transition line is not sensitive to droplet size. Yan et al. [31] investigated the transition of droplet wetting states induced by surface roughness in the gallium-carbon system. When the surface roughness is greater than 1.8, gallium droplets are in the Cassie state, whereas when the surface roughness is less than 1.6, gallium droplets are in the Wenzel state. The aforementioned studies indicate that the wetting state of droplets on structured surfaces is closely related to structure height, spacing, roughness, and other factors.

As a low surface tension fluid [32], maintaining a stable CO_2 droplet state and conducting contact angle measurement experiments in low-temperature environments is extremely challenging, and there have been no relevant experimental data reported so far. Fortunately, with the advancement of computer science, molecular dynamics (MD) simulation, as a powerful tool for studying nanoscale processes and mechanisms [33], has been effectively used for in-depth research into the wetting behavior of droplets at the nanoscale [34]. Yaghoubi et al. [35] used MD simulation methods to create grooves of different depths and widths on graphite substrates to study the effect of surface roughness on the wettability behavior of nanodroplets. Wu et al. [36] used MD simulation to study for the first time the wetting behavior of CO_2 droplets on smooth solid surfaces, and the results indicated that the contact angle of condensed CO_2 droplets is significantly influenced by energy interaction parameters. Yin et al. [37] used MD simulation to investigate the wetting characteristics of CO_2 droplets on smooth and randomly rough substrate surfaces. The capillary drying of liquid CO_2 molecules in the structural gaps at the three-phase contact line of the droplet results in an increase in contact angle with increasing surface roughness density, transforming a CO_2-philic surface into a CO_2-phobic surface.

In previous work, we have investigated the wetting and condensation characteristics of CO_2 droplets on smooth solid surfaces [14],[15]. Building on this, this paper focuses on how to adjust the wetting characteristics of CO_2 droplets on solid surfaces. Enhancing surface microstructures is a common method to regulate wetting performance [38]. Thus, understanding the wetting state of CO_2 droplets on various nanosurfaces and structures is of significant practical importance. In view of the current lack of experimental data on the contact angles of CO_2 droplets on different material surfaces, we simulated the wetting behavior of CO_2 droplets on various material surfaces by adjusting the interaction strength between CO_2 and the surface atoms. This study constructed three types of nanostructures on smooth substrates and simulated the wetting behavior of CO_2 droplets on various structured surfaces. By adjusting the structure size and surface configuration, the regulatory effects of nanostructures on the wetting characteristics of CO_2 droplets were studied. These findings are expected to help us understand the impact of nanostructured surfaces on CO_2 wettability, providing guidance for optimizing the materials and surface structure design for CO_2 condensation, thus improving CO_2 liquefaction efficiency.

2. MODELS AND METHODS

As shown in Fig. 1, the MD simulation system for droplet wetting consists of a solid structured surface and a nano CO_2 droplet, with the structured surfaces composed of arrays of square pillars, grooves, and cylinders. Taking the nano square pillar structure surface as an example, in the simulation system, a spherical CO_2 droplet is positioned above the nano structured surface, with the droplet center 53.87 Å from the Cu substrate. The dimensions of the simulation domain are 160 × 160 × 100 Å^3, with an initial droplet radius of 40 Å, composed of 4000 CO_2 molecules. The structured surface is composed of Cu atoms arranged in an FCC lattice structure with a lattice constant of 3.61 Å. Due to the attraction of the substrate, the CO_2 droplet will gradually deposit on the nano structure and reach equilibrium. For boundary conditions, periodic boundaries are applied in the *x* and *y* directions, and non-periodic boundaries with reflective walls are used in the *z* direction.

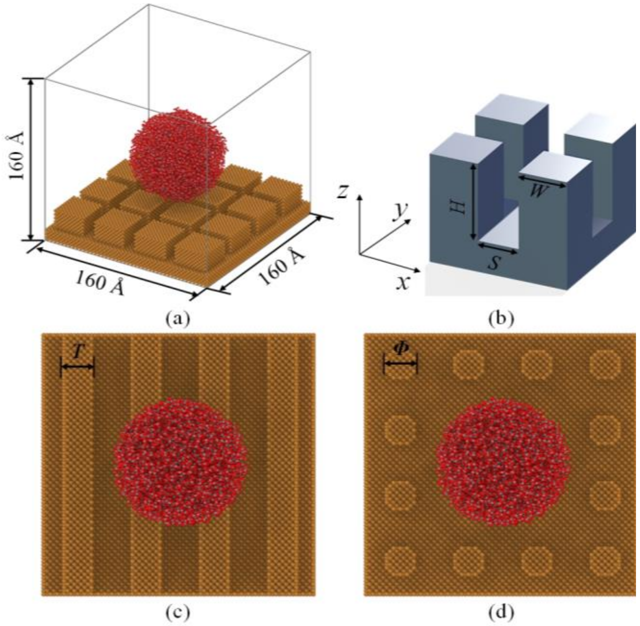

Fig. 1. MD simulation system

The TraPPE_flex model is used to simulate the interactions between CO_2 molecules. This model can effectively describe the gas-liquid equilibrium properties and surface tension of CO_2, as well as other physical parameters [39]. In the TraPPE_flex model, the interaction potential energy is expressed as follows:

$$U_{ij} = 4\varepsilon_{ij}\left[\left(\frac{\sigma_{ij}}{r_{ij}}\right)^{12} - \left(\frac{\sigma_{ij}}{r_{ij}}\right)^{6}\right] + \frac{q_i q_j}{4\pi\varepsilon_0 r_{ij}} + \frac{1}{2}k_\mathrm{b}\left(l_\mathrm{b} - l_\mathrm{b0}\right)^2 + \frac{1}{2}k_\theta\left(\theta - \theta_0\right)^2 \tag{1}$$

where r_{ij} represents the distance between atom pairs *i* and *j*, ε_{ij} represents the depth of the LJ potential well, σ_{ij} represents the distance between atoms when the LJ potential is zero, q_i and q_j represent the charges carried by the atoms, ε_0 represents the vacuum permittivity, and the force constants k_b and k_ϑ are used to describe bond elasticity and bond angle bending.

The interaction between CO_2 and solid atoms is described by the LJ 12-6 potential, and the interaction parameters are calculated using the Lorentz-Berthelot mixing rules [40].

$$\sigma_\text{Cu-C} = \frac{\sigma_\text{Cu} + \sigma_\text{C}}{2}, \varepsilon_\text{Cu-C} = \alpha\sqrt{\varepsilon_\text{Cu} \times \varepsilon_\text{C}} \tag{2}$$

$$\sigma_\text{Cu-O} = \frac{\sigma_\text{Cu} + \sigma_\text{O}}{2}, \varepsilon_\text{Cu-O} = \alpha\sqrt{\varepsilon_\text{Cu} \times \varepsilon_\text{O}} \tag{3}$$

where σ_C = 2.800 Å, ε_C = 0.0536 kcal/mol, σ_O = 3.050 Å, ε_O = 0.1569 kcal/mol, σ_Cu = 2.616 Å, ε_Cu = 4.72 kcal/mol [41]. α is the solid-liquid interaction coefficient, indicating the relative magnitude of the material's surface energy. The larger the value of α, the higher the surface energy of the substrate, and the more CO_2-philic the surface. Therefore, by changing α, the interaction strength between the solid and fluid can be adjusted, thus achieving control over wettability.

In this study, LAMMPS [42] was used for MD simulations, and OVITO [43] was used for visualizing the simulation results. The simulation includes three processes: energy minimization, equilibration, and dynamic calculation. In the energy minimization phase, the initial model was optimized using the conjugate gradient method. In the equilibration phase, the NVT ensemble was applied to the entire system, and the system temperature was controlled to stabilize at 220 K using a Nose-Hoover thermostat. To prevent the drift and vibration of Cu atoms, the atoms on the structured surface were fixed near their equilibrium positions. Subsequently, the NVT ensemble was removed, and the NVE ensemble was used for the integration calculation of the CO_2 droplet. Long-range Coulomb interactions were calculated using the PPPM method with an accuracy of 10^{-4} and a time step of 1 fs.

3. RESULTS AND DISCUSSION

3.1 *The influence of interaction strength on droplet wetting*

This section mainly investigates the effect of the solid-liquid interaction coefficient α on the CO_2 wetting process on a structured surface with a square pillar spacing S of 13.685 Å and a pillar height H of 15.195 Å. As a control group, the wetting process of CO_2 droplets on a smooth solid surface with the same α values was also simulated. α was set to 0.06, 0.08, 0.10, 0.12, 0.14, and 0.16, to transition the smooth solid surface from CO_2-phobic to CO_2-philic.

Simulation results show that the wetting process can be divided into three stages: in the first stage, the CO_2 droplet gradually approaches the solid structured surface under the influence of Coulomb and short-range forces; in the second stage, the CO_2 droplet begins to infiltrate into the gaps between the square pillars; in the third stage, the CO_2 droplet reaches a stable state, characterized as either the Wenzel state or the Cassie state. The final wetting morphologies of CO_2 droplets on the square pillar structured surface for different α values are shown in Fig. 2.

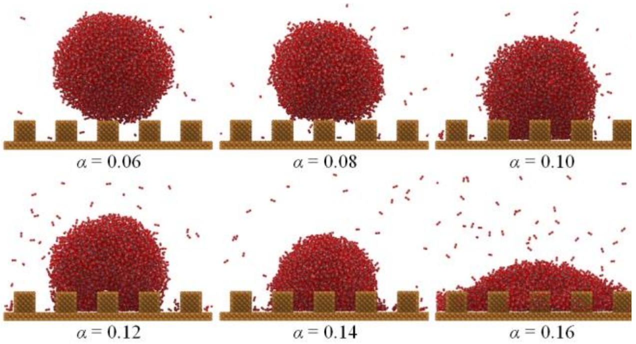
$\alpha = 0.06$ $\alpha = 0.08$ $\alpha = 0.10$

$\alpha = 0.12$ $\alpha = 0.14$ $\alpha = 0.16$

Fig. 2. Wetting morphologies of CO_2 droplets on the square pillar structured surfaces

The simulation results show that the contact area between the CO_2 droplet and the tops of the pillars varies with α. When α is between 0.06 and 0.08, the CO_2 droplet exhibits a spherical cap morphology above the square pillar structured surface, tending more towards the Cassie state. When α increases to 0.10, although the droplet still exhibits a spherical cap morphology on the pillar surface, it can partially infiltrate into the grooves between the square pillars, beginning to show the Wenzel state. When α further increases to 0.16, the droplet gradually spreads over the structured surface, with CO_2 completely infiltrating into the grooves, and the square pillar structured surface is fully wetted by the CO_2 droplet. At the same interaction strength, the droplet exhibits different wetting morphologies and contact angle characteristics on smooth and structured surfaces.

Fig. 3 shows the two-dimensional density contour plots of CO_2 droplets on square pillar structured surfaces with different wetting properties. As α increases, the Cu-CO_2 interaction strength increases, making the droplets more easily attracted to the CO_2-philic structured surface. When α is 0.12 and 0.14, although the smooth surface already exhibits CO_2-philic properties, the spherical cap morphology on the square pillar structured surface still shows CO_2-phobic effects, with weaker wetting than the smooth solid surface. When α is 0.14, a significant layered high-density region is observed in the density contour plot, with the surface adsorbing multiple layers of CO_2 molecules. Therefore, changing the interaction strength also alters the density distribution and adsorption layer structure of the droplets on the structured surface.

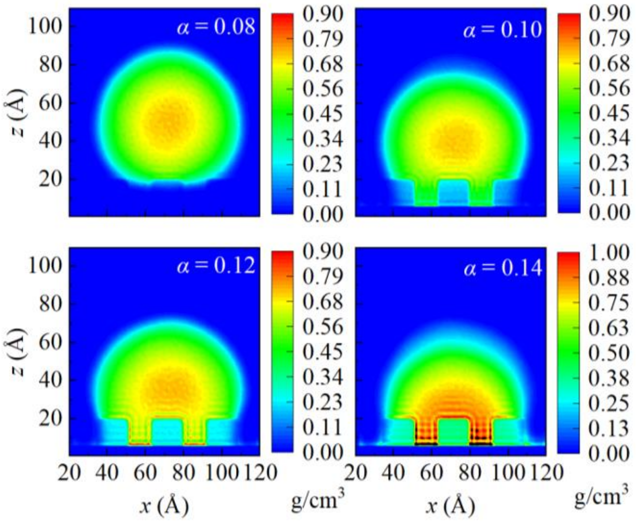

Fig. 3. Representative density contour plots of Droplets on the square pillar structured surfaces

As shown in Fig. 4, the distribution of droplet density along the z-direction reveals that with the decrease in interaction coefficient, the number of peaks in the droplet density along the z-axis significantly decreases, and the plane density of the adsorption layer decreases, which is consistent with the pattern observed on smooth surfaces. Compared to smooth surfaces, when α is small and the surface exhibits CO_2-phobic properties, the number of adsorption layers and the density of adsorption layers of CO_2 droplets on the structured surface are lower. This is mainly due to the smaller contact area between the droplet and the solid surface, which reduces the interaction energy between the solid surface and the droplet, resulting in a smaller increase in the local CO_2 density near the pillar surface. This implies that the square pillar structure can further enhance the

CO_2-phobic properties of CO_2-phobic surfaces. The number of CO_2 layers near the pillar structure surface is less than that near the smooth surface. However, in the region below the pillar structure surface where $z < 20$ Å, the CO_2 density is higher than that of gaseous CO_2, corresponding to the partial infiltration of the suspended droplet into the grooves between the pillars.

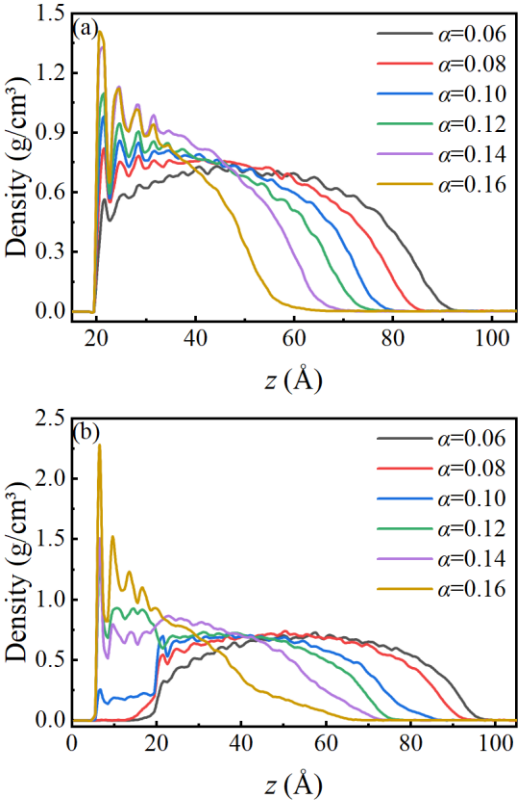

Fig. 4. CO_2 Density distribution along the *z*-direction on solid surfaces. (a) Smooth solid surface. (b) Square pillar structured surface

Fig. 5 shows the variation of CO_2 droplet contact angle on smooth and structured surfaces with interaction strength. It can be seen from the figure that when the interaction coefficient α increases from 0.06 to 0.16, the contact angle of droplets on the structured surface monotonically decreases from 160° to 55°, which is consistent with the pattern observed on the smooth surface. However, under the same α condition, the contact angle on the structured surface is always greater than that on the smooth surface, demonstrating the potential of the structured surface to enhance CO_2-phobic properties. Moreover, when α = 0.14, the transformation from CO_2-philic to CO_2-phobic surface can be achieved by applying pillar structures to the smooth solid surface. Therefore, the wettability of liquid CO_2 on solid surfaces can be fine-tuned by constructing pillar structures.

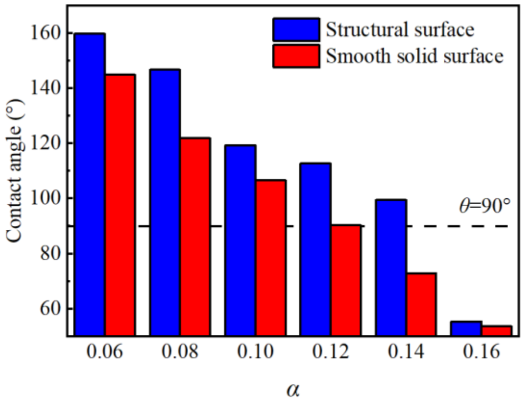

Fig. 5. Variation of droplet contact angle on smooth and structured surfaces

3.2 *The effect of square pillar structural parameters on wetting behavior*

The height of the square pillar structure is *H*, the side length is *W*, and the spacing between pillars is *S*. The solid fraction of the structured surface can be expressed as $F = W^2/(S+W)^2$. To study the effect of geometric parameters of the square pillar structure on CO_2 droplet wetting, different solid fractions *F* (56.25%, 42.25%, 30.25%, 20.25%) and different heights *H* (10.8 Å, 14.4 Å, 18.0 Å, 21.6 Å, 25.2 Å) of the nanostructured surface were designed, with $S + W = 40$ Å. Since the focus of this section is on how to adjust the wetting state of CO_2 droplets, it is necessary to ensure the transition of the droplet wetting state within the studied range of structural parameters. Through simulation in section 3.1, the optimal value of α was found to be 0.08. The wetting state of CO_2 droplets on different structured surfaces is shown in Fig. 6.

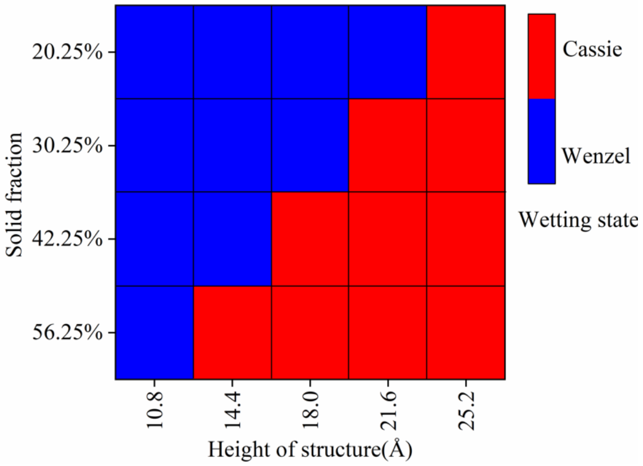

Fig. 6. Wetting states of droplets on different nanostructures

When the solid fraction is constant, the higher the structure height, the stronger the CO_2-phobic nature of the surface, and the wetting state tends towards the

Cassie state. When the structure height is constant, the smaller the solid fraction, the stronger the CO_2-philic nature of the surface, and the wetting state tends towards the Wenzel state. Therefore, the solid fraction F and the pillar height H show a synergistic effect in determining the final wetting state of CO_2.

As illustrated in Fig. 7(a), when the droplet is in the Cassie wetting state, a decrease in the solid fraction of the square column surface leads to a reduction in the contact area between the CO_2 droplet and the structured surface, thereby lowering the interaction energy between the CO_2 droplet and the structured surface. However, when the decrease in the solid fraction of the square column surface causes the CO_2 droplet to transition from the Cassie state to the Wenzel state ($F_{1\text{-}3}H_4$ vs. F_4H_4), the contact area between the CO_2 droplet and the structured surface suddenly increases, thus significantly increasing the interaction energy between the CO_2 droplet and the structured surface, which is higher than the solid-liquid interaction energy in all Cassie states.

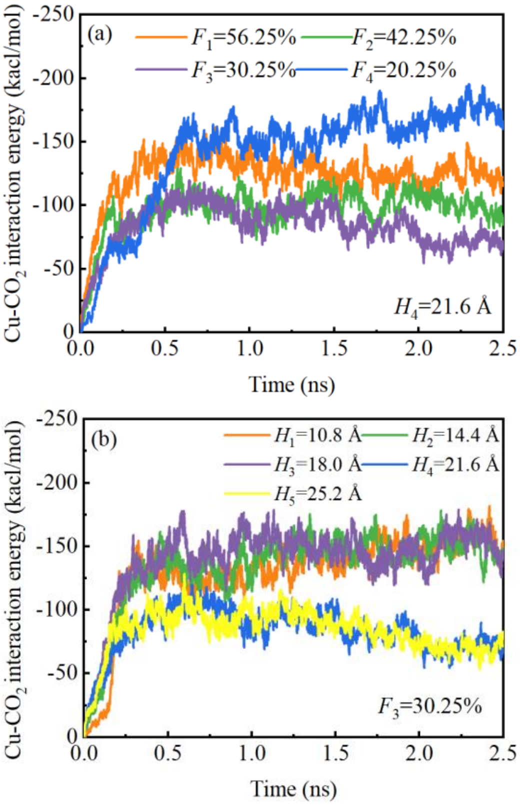

Fig. 7. Interaction energy between the solid surface and CO_2. (a) Different F. (b) Different H

Similarly, as depicted in Fig. 7(b), when the droplet is in the Wenzel wetting state ($F_3H_{1\text{-}3}$), an increase in the height of the square column results in almost no change in the contact area between the CO_2 droplet and the structured surface, thus the interaction energy between the CO_2 droplet and the structured surface does not show a significant change. When the droplet is in the Cassie state ($F_3H_{4\text{-}5}$), an increase in the height of the square column results in almost no change in the contact area between the CO_2 droplet and the structured surface, thus the interaction energy between the CO_2 droplet and the structured surface also remains unchanged. However, when an increase in the height of the structure causes the CO_2 droplet to transition from the Wenzel state to the Cassie state, the contact area between the CO_2 droplet and the structured surface suddenly decreases, thus the interaction energy between the CO_2 droplet and the structured surface suddenly decreases, and is lower than the solid-liquid interaction energy in all Wenzel states. Therefore, when an increase in the solid fraction or the height of the structure causes the CO_2 droplet to transition from the Wenzel state to the Cassie state, the interaction energy between CO_2 and the structured surface significantly decreases.

The contact angles of CO_2 droplets on 20 different structured surfaces were calculated, and the results are shown in Fig. 8. The contact angle varies with the change in structural size. Compared to a smooth surface, the static contact angle of CO_2 droplets on the solid surface increases with the addition of square pillar microstructures, indicating that the square pillar microstructures enhance the CO_2-phobicity of the substrate surface. Combining the wetting state results in Fig. 7, it can be seen that when the droplets remain in the Wenzel state or Cassie state, changes in the square pillar structure parameters do not cause significant changes in the static contact angle. However, when changes in structure height and solid fraction cause the droplets to transition from the Wenzel state to the Cassie state, the static contact angle of CO_2 droplets increases significantly. For the square pillar structures, although

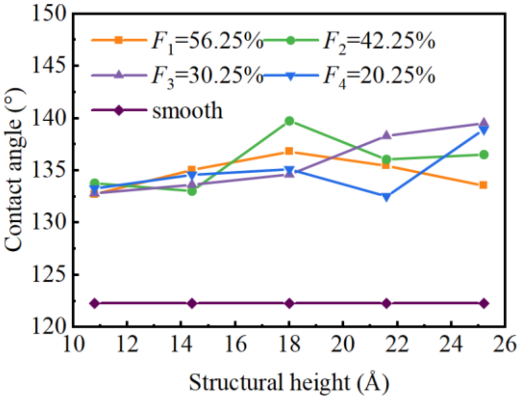

Fig. 8. Variation of CO_2 droplet contact angles on different structured surfaces

increasing the pillar height or the solid fraction can both cause the wetting state of CO_2 droplets to transition from the Wenzel state to the Cassie state, the contact angle does not change uniformly with changes in pillar height and solid fraction.

3.3 The influence of surface structure configuration on droplet wetting

To investigate whether the wetting behavior of CO_2 droplets varies with surface configuration, three types of structured surfaces were set with different structure heights and spacings to simulate the wetting states of CO_2 droplets. The structure spacings S were set to 11.88 and 19.10 Å, and the structure heights H ranged from 4.365 to 18.805 Å. In addition, the square pillar structure had a side length W, the groove structure had a spacing T, and the cylinder structure had a diameter Φ, all equal to 17 Å. The coefficient α was set to 0.08, resulting in the Cu substrate exhibiting CO_2-phobicity.

As shown in Fig. 9, with the same structure spacing, as the structure height increases, CO_2 droplets on all three surfaces transition from Wenzel to Cassie wetting states. When the structure spacing S is 11.88 Å (Fig. 9a), CO_2 droplets exhibit a partially wetting (PW) state on the groove and pillar surfaces, which is an intermediate transition state from Wenzel to Cassie states. The reason for the different states of the droplets lies in the change in interaction between CO_2 molecules and substrate atoms, leading to competition between supporting force, attraction force, and the vertical component of interfacial tension. At lower structure heights, the distance between the droplet and the substrate is smaller, hence the attraction force is maximized. This results in the Wenzel state for CO_2 droplets. With increasing structure height, the attraction and supporting forces decrease, allowing the vertical component of interfacial tension to dominate. Therefore, the droplet transitions from the Wenzel state to the Cassie state. When the structure spacing S is increased to 19.10 Å (Fig. 9b), the interaction force between CO_2 molecules and substrate atoms increases compared to S = 11.88 Å, requiring further increases in structure height to allow the vertical component of interfacial tension to dominate, thus transitioning CO_2 droplets from the Wenzel to the Cassie state.

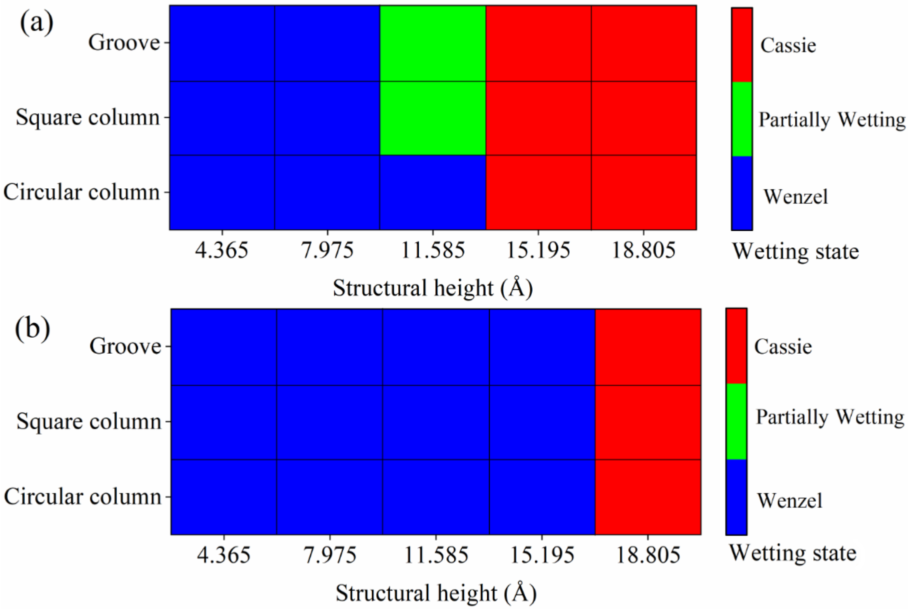

Fig. 9. Wetting states of CO_2 droplets on structured surfaces. (a) S = 11.88 Å. (b) S = 19.10 Å

As shown in Fig. 10, the static contact angles of CO_2 droplets on three different configurations of rough surfaces were calculated.

Compared to smooth solid surfaces, the static contact angles of CO_2 droplets on various microstructured surfaces all increase, indicating that microstructures enhance the CO_2-phobicity of the substrate surface. It can be observed that when CO_2 droplets remain in the Wenzel or Cassie states, the static contact angle changes are not significant. However, when changes in structure size cause a transition in wetting states, the static contact angle undergoes noticeable changes. Taking the cylindrical structure surface as an example, as the wetting state transitions from Wenzel to Cassie (at S = 11.88 Å, H ranges from 11.585 Å to 15.195 Å; at S = 19.10 Å, H ranges from 15.195 Å to 18.805 Å), the static contact angle of the droplet significantly increases. Additionally, it was observed that when $W = T = \Phi$, the contact angles of CO_2

nanodroplets on three different rough surface configurations are similar.

4. CONCLUSIONS

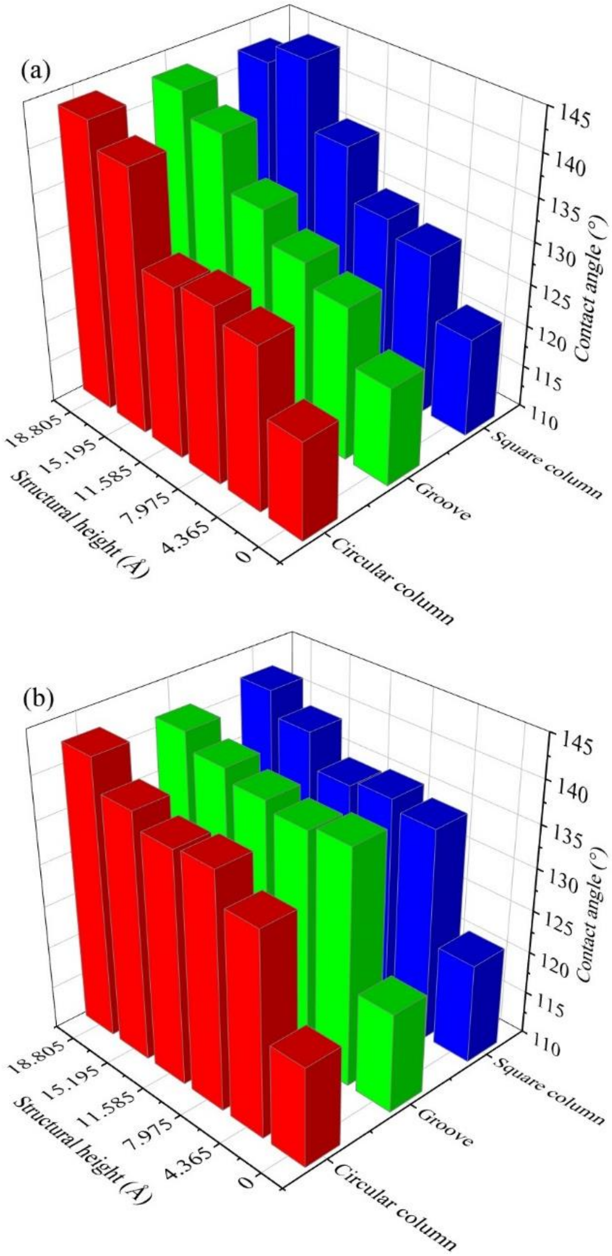

Fig. 10. Contact angles of CO_2 droplets on structured surfaces. (a) S = 11.88 Å. (b) S = 19.10 Å

The determination of the regulatory role of nanostructures in controlling the wetting behavior of CO_2 droplets holds significant practical implications for advancing CCUS technologies. This study, based on molecular dynamics simulations, investigated the impact of nanostructures on the wetting properties of CO_2 droplets by adjusting the strength of solid-liquid interactions, nanostructure dimensions, and surface configurations. The main conclusions of this study are as follows:

(1) The wetting behavior of CO_2 droplets on solid surfaces can be finely tuned by constructing pillar-like structures. Under the same α conditions, the contact angle on structured surfaces is greater than that on smooth surfaces. Specifically, when α = 0.14, treating a smooth solid surface with pillar-like structures can achieve a transition from CO_2-philic to CO_2-phobic surfaces, demonstrating the potential of pillar structures to enhance surface CO_2-phobicity. Furthermore, by varying the interaction parameter α, that is, adjusting the surface energy of the substrate, the wetting state of CO_2 droplets transitions from the Cassie state to the Wenzel state.

(2) For square pillar structures, when the structure height is constant, a smaller solid fraction enhances surface CO_2-philicity, leading to a tendency towards the Wenzel state in the wetting state of droplets. With a fixed solid fraction, increasing structure height enhances surface CO_2-phobicity, leading to a tendency towards the Cassie state in the wetting state. When CO_2 droplets transition from the Wenzel state to the Cassie state, the interaction energy between CO_2 and the structured surface significantly decreases.

(3) For a given interaction parameter α = 0.08, due to the reduced liquid-solid contact area of the droplet, the interaction between the droplet and the solid substrate weakens, significantly increasing the contact angle on the square pillar structure surface. Moreover, when changes in structure height and solid fraction cause the droplet to transition from the Wenzel state to the Cassie state, the static contact angle of CO_2 droplets increases significantly.

(4) Three types of structured surfaces were constructed using square pillars, cylinders, and grooves as structural units. These surface configurations all play an equal role in adjusting the wetting state of CO_2 droplets. Furthermore, the addition of different surface microstructures increases the contact angle of CO_2 droplets, enhancing the CO_2-phobicity of the substrate in various configurations.

ACKNOWLEDGEMENT

The project is supported by National Natural Science Foundation (Number U21B2087). Thanks to my girlfriend, Zhang Yuanyuan, for her support.

DECLARATION OF INTEREST STATEMENT

The authors declare that they have no known competing financial interests or personal relationships that could have appeared to influence the work reported in this paper. All authors read and approved the final manuscript.

REFERENCE

[1] Wen C, Li B, Ding H, Akrami M, Zhang H, Yang Y. Thermodynamics analysis of CO_2 condensation in supersonic flows for the potential of clean offshore natural gas processing. Applied Energy 2022;310: 118523.

[2] Chen J, Wang T, Li A, Gao YY, Huang Z, Jiang W, et al. Influence of inner wall roughness of supersonic separator on non-equilibrium condensation of CO_2 benefiting flue gas decarbonization. Journal of Cleaner Production 2024;434:139964.

[3] Krevor S, de Coninck H, Gasda SE, Ghaleigh NS, de Gooyert V, Hajibeygi H, et al. Subsurface carbon dioxide and hydrogen storage for a sustainable energy future. Nature Reviews Earth & Environment 2023;4:102–18.

[4] Wang Y, Wang R, Tanaka K, Ciais P, Penuelas J, Balkanski Y, et al. Accelerating the energy transition towards photovoltaic and wind in China. Nature 2023;619:761–7.

[5] Karimi M, Shirzad M, Silva JAC, Rodrigues AE. Carbon dioxide separation and capture by adsorption: a review. Environmental Chemistry Letters 2023;21:2041-2084.

[6] Ding H, Zhang Y, Dong Y, Wen C, Yang Y. High-pressure supersonic carbon dioxide (CO_2) separation benefiting carbon capture, utilisation and storage (CCUS) technology. Applied Energy 2023;339:120975.

[7] Dziejarski B, Krzyżyńska R, Andersson K. Current status of carbon capture, utilization, and storage technologies in the global economy: A survey of technical assessment. Fuel 2023;342:127776.

[8] Mon MT, Tansuchat R, Yamaka W. CCUS Technology and Carbon Emissions: Evidence from the United States. Energies 2024;17:1748.

[9] Xin Y, Zhang Y, Xue P, Wang K, Adu E, Tontiwachwuthikul P. The optimization and thermodynamic and economic estimation analysis for CO_2 compression-liquefaction process of CCUS system using LNG cold energy. Energy 2021;236:121376.

[10] Jackson S, Brodal E. Optimization of the CO_2 liquefaction process-performance study with varying ambient temperature. Applied Sciences 2019;9:4467.

[11] Al Baroudi H, Awoyomi A, Patchigolla K, Jonnalagadda K, Anthony EJ. A review of large-scale CO_2 shipping and marine emissions management for carbon capture, utilisation and storage. Applied Energy 2021;287:116510.

[12] Dlamini GM, Fosbøl PL, Ness K, Remiezowicz E, Losnegård SE, von Solms N. Optimisation of carbon dioxide pressurisation pathways for pipeline offshore delivery. International Journal of Greenhouse Gas Control 2023;128:103943.

[13] Han C, Zahid U, An J, Kim K, Kim C. CO_2 transport: Design considerations and project outlook. Current Opinion in Chemical Engineering 2015;10:42–8.

[14] Cao H, Cao X, Cai W, Zhao X, Guo D, Ding G, et al. Exploring the effect of surface wettability on heterogeneous condensation of carbon Dioxide: A molecular dynamics study. Journal of Molecular Liquids 2023;388:122693.

[15] Cao HG, Cao XW, Zhao XY, Ma YQ, Dong MQ, Li H, et al. Wetting behavior of CO_2 droplets on smooth solid surface: molecular simulation perspective. Journal of Physics: Conference Series 2023;2594:012048.

[16] Cao H, Wang Z, Shi Y, Cao X, Cai W, Bian J. Enhancing carbon capture: Exploring droplet wetting and gas condensation of carbon dioxide on nanostructured surfaces. Journal of Cleaner Production 2024;454:142343.

[17] Hubao A, Yang Z, Hu R, Chen YF. Molecular origin of wetting characteristics on mineral surfaces. Langmuir 2023;39:2932–42.

[18] Xing L, Zhang Q, Fu Q, Yu J, Huang X. Preparation and properties of polytetrafluoroethylene superhydrophobic surface. Colloids and Surfaces A: Physicochemical and Engineering Aspects 2023;670:131574.

[19] Tang S, Li Q, Yu Y, Qiu Y. Enhancing dropwise condensation on downward-facing surfaces through the synergistic effects of surface structure and mixed wettability. Physics of Fluids 2021;33:083301.

[20] Zhu GP, Li XA, Wang QY, Fang MH, Ding YC. Electric manipulation on deformation of ionic ferrofluid sessile droplets. Electrophoresis 2024;45:1243-1251.

[21] Xu J, Jia L, Dang C, Ding Y, Liu X. Wetting behavior of nanodroplets with low surface tension on pillar-type nanostructured substrates: Molecular dynamics simulations. Journal of Molecular Liquids 2024;393:123581.

[22] Meena MK, Sinhamahapatra A, Kumar A. Superhydrophobic polymer composite coating on glass via spin coating technique. Colloid And Polymer Science 2019;297:1499–505.

[23] Ren J, Duan F. Recent progress in experiments for sessile droplet wetting on structured surfaces. Current Opinion in Colloid and Interface Science 2021;53:101425.

[24] Liu H, Liu D, Li P, Zeng Y, Jin H. Direct observation of the wetting state of Cassie and Wenzel. Materials Letters 2023;340:134182.

[25] Gao S, Liao Q, Liu W, Liu Z. Effects of solid fraction on droplet wetting and vapor condensation: A molecular dynamic simulation study. Langmuir 2017;33:12379–88.

[26] Hao PF, Lv CJ, Yao ZH, Niu FL. Wetting property of smooth and textured hydrophobic surfaces under condensation condition. Science China-Physics Mechanics & Astronomy 2014;57:2127–32.

[27] Wang Q, Xie H, Liu J, Liu C. Heterogeneous nucleation of argon vapor on the nanostructure surface with molecular dynamics simulation. Journal of Molecular Graphics and Modelling 2020;100:107674.

[28] Wang X, Jia L, Dang C. The wetting transition of low surface tension droplet on the special-shaped microstructure surface. Colloids and Interface Science Communications 2022;50:100649.

[29] Al Balushi KM, Sefiane K, Orejon D. Binary mixture droplet wetting on micro-structure decorated surfaces. Journal of Colloid and Interface Science 2022;612:792–805.

[30] Wu XH, Yang Z, Duan YY. Molecular Dynamics Analysis on the Wetting Properties of R32, R1234yf, and Their Mixture on Pillar-Type Nanostructured Substrates. LANGMUIR 2020;36:55–63.

[31] Yan M, Li T, Zheng P, Wei R, Jiang Y, Li H. Wetting state transition of a liquid gallium drop at the nanoscale. Physical Chemistry Chemical Physics 2020;22:11809–16.

[32] Snustad I, Røe IT, Brunsvold A, Ervik Å, He J, Zhang Z. A review on wetting and water condensation - Perspectives for CO_2 condensation. Advances in Colloid and Interface Science 2018;256:291–304.

[33] Cao H, Cao X, Li H, Zhao X, Cai W, Guo D, et al. Nucleation and condensation characteristics of carbon dioxide in natural gas: A molecular simulation perspective. Fuel 2023;342:127761.

[34] Cai W, He Z, Wang J, Wang Z, Li Q, Wang Y. Wetting characteristics of ethane droplet – A molecular dynamics study. Journal of Molecular Liquids 2023;371:121115.

[35] Yaghoubi H, Foroutan M. Molecular investigation of the wettability of rough surfaces using molecular dynamics simulation. Physical Chemistry Chemical Physics 2018;20:22308–19.

[36] Wu J, Ervik Å, Snustad I, Xiao S, Brunsvold A, He J, et al. Contact angle and condensation of a CO_2 droplet on a solid surface. Journal of Physical Chemistry C 2019;123:443–51.

[37] Yin Y, Zhao L, Lin S. CO_2-philicity to CO_2-phobicity Transition on Smooth and Stochastic Rough Cu-like Substrate Surfaces. Langmuir 2023;39:17818–29.

[38] Chen L, Wang SY, Xiang X, Tao WQ. Mechanism of surface nanostructure changing wettability: A molecular dynamics simulation. Computational Materials Science 2020;171:109223.

[39] Perez-Blanco ME, Maginn EJ. Molecular dynamics simulations of carbon dioxide and water at an ionic liquid interface. Journal of Physical Chemistry B 2011;115:10488–99.

[40] DELHOMMELLE J, MILLIÉ P. Inadequacy of the Lorentz-Berthelot combining rules for accurate predictions of equilibrium properties by molecular simulation. Molecular Physics 2001;99:619–25.

[41] Heinz H, Vaia RA, Farmer BL, Naik RR. Accurate simulation of surfaces and interfaces of face-centered cubic metals using 12-6 and 9-6 lennard-jones potentials. Journal of Physical Chemistry C 2008;112:17281–90.

[42] Plimpton S. Fast Parallel Algorithms for Short-Range Molecular Dynamics. Journal of Computational Physics 1995;117:1–19.

[43] Stukowski A. Visualization and analysis of atomistic simulation data with OVITO-the Open Visualization Tool. Modelling and Simulation in Materials Science and Engineering 2010;18.